

Article

Tracing the Sources and Processes of Groundwater in an Alpine Glacierized Region in Southwest China: Evidence from Environmental Isotopes

Yuchuan Meng ^{1,*}, Guodong Liu ¹ and Mingxi Li ²

¹ State Key Laboratory of Hydraulics and Mountain River Engineering, College of Water Resource and Hydropower, Sichuan University, Chengdu 610065, China; E-Mail: SDXY_GDL@126.com

² Department of Hydropower Business, Power China Huadong Engineering Corporation Limited, No. 22, ChaoWang Rd., Hangzhou 310014, China; E-Mail: li_mx@ecidi.com

* Author to whom correspondence should be addressed; E-Mail: mengyuchuan@126.com; Tel.: +86-28-8546-3699.

Academic Editor: David Polya

Received: 15 February 2015 / Accepted: 21 May 2015 / Published: 29 May 2015

Abstract: The melting of alpine snow and glaciers is an important hydrologic process on Mount Gongga, China. The relevance of ice-snow melt to the groundwater recharge in the glacierized Hailuoguo watershed is so far not well known. To better understand the origin of groundwater and the hydrological interactions between groundwater, meltwater, and precipitation in this region, 148 environmental isotopic data of water samples were analyzed for changes in isotopic composition. The results indicate that the groundwater contains a uniform isotopic signature, with $\delta^{18}\text{O}$ values between -13.5‰ and -11.1‰ and $\delta^2\text{H}$ values between -90‰ and -75‰ . The mean stable isotopic composition of groundwater is heavier than that of ice-snow meltwater but lighter than that of precipitation. The effect of evaporation on the isotopic variation of groundwater is very limited and the seasonal isotope variations in precipitation are attenuated in groundwater. A model based on the $\delta^{18}\text{O}$ results suggests that approximately 35% of the groundwater is derived from ice-snow meltwater sources. The study demonstrates that ice-snow meltwater is a substantial source of shallow groundwater in the alpine regions on the edge of the Tibetan Plateau.

Keywords: Hailuoguo watershed; groundwater; ice-snow meltwater; stable isotope

1. Introduction

In many high-elevation mountain areas, ice and snow are an essential component of the hydrological cycle, and the seasonal character and amount of runoff are closely linked to cryospheric processes [1]. Significant climate change is already globally visible, and is expected to become more pronounced in the future [2]. Earth's mean surface temperature has increased by approximately 1 °C since the beginning of the 20th century [3], and the temperature has increased by 0.4–0.5 °C from 1860 to 2005, most drastically after 1951, in China [4]. Through increases in temperature are coupled with changes in precipitation regimes, mountain regions seem to be particularly sensitive to the changing climate [5,6]. Due to their sensitivity to temperature and precipitation, mountain glaciers and snow covers have lost a considerable amount of their area and volume [7,8], and a further rise in temperature will exacerbate this situation [9]. Climatic changes will significantly affect melt features in mountainous areas [10,11]. As glaciers and snow covers rapidly melt, they will provide enhanced runoff, but as they diminish, the runoff will decline to levels that simply reflect precipitation [12–15].

The hydrological regimes have been seriously affected by the changes in glaciation and snow cover on the Tibetan Plateau [16]. As the highest mountain on the eastern margin of the Tibetan Plateau, Mount Gongga is the largest area of modern glaciation in the Hengduan Mountains and one of the principal glacierized areas controlled by the monsoonal climate in the southwest of China. Owing to the distinct characteristics of this alpine region, including its diverse topography, geology, climate, and hydrology, it has hosted many scientific investigations [17–21]. Located on the eastern slope of Mount Gongga, Hailuoguo (HLG) watershed is an ideal location for studying the distinctive hydrologic regimes of this alpine area. To develop a baseline assessment of the components and the generation mechanism of groundwater in this headwater region, data on isotope hydrology have been generated almost monthly between May 2008 and November 2009.

Craig (1961) observed the following correlation between the stable isotope ratios of hydrogen and oxygen in precipitation: $\delta^2\text{H} = 8\delta^{18}\text{O} + 10$, which was later defined as the global meteoric water line (GMWL). The slope of the GMWL, 8, is controlled by the ratio between the isotope equilibrium fractionation factors of oxygen and hydrogen, while the intercept of 10 is controlled by evaporation processes in the water vapor source region [22]. Rozanski *et al.*, (1993) published a refined GMWL, $\delta^2\text{H} = 8.20\delta^{18}\text{O} + 11.27$, which was derived from the IAEA/WMO GNIP (the Global Network of Isotopes in Precipitation maintained by the International Atomic Energy Agency and the World Meteorological Organization) database [23]. Local meteoric water lines (LMWL) are controlled by local geographic and meteorological factors. Hence, the LMWL at any given location might be quite different from the GMWL.

Environmental isotopes play an important role in studies of the groundwater provenance and recharge mechanisms in the pro-glacial groundwater system. Such investigations include the studies of Kristiansen *et al.*, (2013) in front of a warm-based glacier in Southeast Greenland [24], Wadham *et al.*, (2007) from the proglacial zone of a retreating high Arctic glacier [25], Blaen *et al.*, (2013) in Arctic river basins [26], and Tan *et al.*, (2009) in the western Qaidam Basin, China [27]. However, these studies of groundwater do not represent the isotopic features of the groundwater in the glacierized HLG watershed. Moreover, previous studies of the groundwater in the HLG watershed have been generally qualitative.

Combined with the available meteorological and hydrological data in the study area, we attempt (1) to understand the seasonal variability of the isotope concentration in groundwater, ice-snow meltwater, and precipitation in the glacierized area; (2) to determine the correlation between $\delta^2\text{H}$ and $\delta^{18}\text{O}$ for water collected during this sampling period; and (3) to estimate the relative contributions of the water components, especially the ice-snow meltwater, to groundwater recharge. We expect that the results will provide insight into water resource and watershed management in alpine glacierized regions.

2. Study Area

Mount Gongga (29°20' N–30°20' N, 101°30' E–102°15' E) is located in the transition zone between the Tibetan Plateau and the South Chinese plains. It is the highest peak, 7556 m a.s.l., in the eastern part of the Tibetan Plateau, and its eastward drop, with a vertical difference of more than 6300 m within a horizontal distance of only 11 km, is one of the largest in the world [28]. The eastern slopes reach down into the Dadu Valley (1100 m a.s.l.), and the western slopes blend into the Tibetan Plateau (3000 to 3500 m a.s.l.). At comparable altitudes, the eastern slopes are colder and more humid than the western slopes. Comparable to other Chinese mountain ranges, the maximum precipitation occurs at far higher altitudes (2900 to 3200 m a.s.l.) along the eastern slope [29]. There are 74 glaciers on the east (33 glaciers) and west (41 glaciers) slopes of Mount Gongga.

The glacier area and volume on the eastern slope are larger than those on the west. The snow-line elevations on the eastern slope, ranging from 4800 to 5000 m a.s.l., are lower than those on the west, which range from 5000 to 5200 m a.s.l. These 74 glaciers have decreased in area by 11.3% (29.2 km²) from 1966 to 2009 [20].

The HLG watershed is situated on the eastern slope of Mount Gongga, ranging from 2756 to 7556 m a.s.l., with a mean altitude of 4714 m a.s.l. Characterized by abundant precipitation, little evaporation, large discharge, and complex water resources, the HLG watershed covers an area of 94.75 km², of which 34.67 km² (36.6%) is glacierized [30]. Belonging to the wet monsoon climate, the alpine region is controlled by the southwest and southeast monsoons in the summer and by the westerly circulation in the winter [31]. The HLG watershed contains seven glaciers, HLG Glacier, HLG Glacier No. 1, HLG Glacier No. 2, and four other smaller glaciers.

HLG Glacier, which covers a total area of approximately 25.7 km² and is approximately 13.1 km in length, is the largest and longest glacier of the 74 glaciers on Mount Gongga [19]; the six other glaciers in the HLG watershed are much smaller. Extending from 7556 m a.s.l. to 2990 m a.s.l. at its terminus, HLG Glacier is a typical monsoonal temperate glacier [32].

3. Data and Methods

3.1. Field Measurements and Sampling

Water samples, including groundwater, precipitation, and ice-snow meltwater, were collected almost monthly from May 2008 to November 2009 and in June 2011 in the study area for analysis of the oxygen and hydrogen isotopic compositions. The sampling site of the precipitation coincides with the meteorological station (3000 m a.s.l.), and the sampling site of section II coincides with the existing HLG River hydrological station (2920 m a.s.l.) (Figure 1).

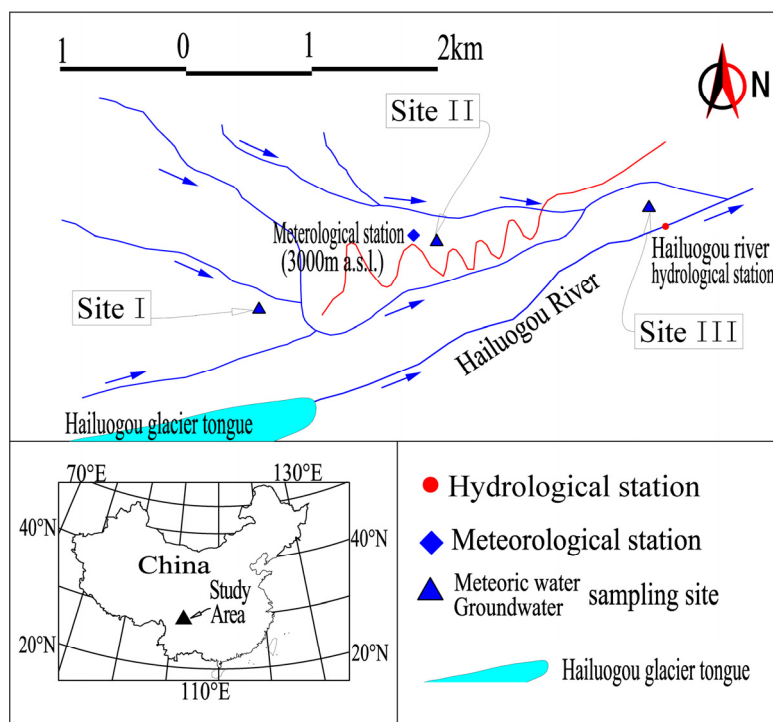


Figure 1. Map of the study region, with the meteorological station (3000 m a.s.l.) and hydrological station (2920 m a.s.l.).

Groundwater was sampled from two existing wells at site I and site III. Prior to sampling, several well volumes were removed to ensure water maximum sample quality. The water samples were passed through 0.45 μm pre-cleaned membrane filters and were collected in 500 mL pre-cleaned high-density linear polyethylene bottles with tight-fitting screw caps. Evaporation through partially filled bottles or leaky bottle caps may pose a problem. Water bottles were filled slowly to minimize post-sampling alterations in the isotopic composition and were immediately stored in ice boxes.

Precipitation was sampled at two locations, site I and site III. During the monitoring programs for precipitation, precautions against evaporation are essential, and event samples are integrated on a monthly basis. A layer of paraffin oil was poured into the sampling container to prevent evaporation. Using a hand auger, the glacier and snowpack were drilled to retrieve cores of ice and snow at the area of the HLG Glacier tongue. Ice-snow samples were sealed in plastic in the field and then left to be melted and bottled.

Water samples must be collected and stored in well-sealed bottles. Repeated sampling for different isotope analyses at the sampling sites will produce a large number of water sample bottles. Unique sequential numbering was used for sample identification, with the specific analysis included, using a narrow-tip waterproof marker or pencil (graphite does not fade) on a sticky label that was then totally covered by clear tape. Sampling for ^{18}O and ^2H in water is simple because neither is measurably affected by chemical or biological processes. The collection bottles were washed at least three times using *in situ* water.

The number of monthly samples varied slightly due to the accessibility of water samples, caused mainly by unfavorable weather conditions. We took two samples at every sampling location in case of failure in the process of sample transportation.

3.2. Laboratory Analysis

These samples were transported with ice bags and refrigerated until use. The isotopic analyses were performed after the sample campaign was completed. The isotopic compositions ($\delta^{18}\text{O}$, $\delta^2\text{H}$) of the samples were determined at the State Key Laboratory of Hydrology-Water Resources and Hydraulic Engineering of Hohai University, China, using a Thermo Finnigan MAT253 mass spectrometer. The stable isotope compositions of hydrogen and oxygen in the water samples are expressed using the conventional delta notation relative to the Vienna standard mean ocean water (V-SMOW), in parts per thousand:

$$\delta(\text{‰}) = \left(\frac{R_{\text{sample}} - R_{\text{standard}}}{R_{\text{standard}}} \right) \times 1000 \quad (1)$$

where R_{sample} and R_{standard} denote the $^{18}\text{O}/^{16}\text{O}$ or $^2\text{H}/^1\text{H}$ ratios in the sample and the standard material, respectively. The standards of both the oxygen and hydrogen isotope measurements are V-SMOW established and distributed by the International Atomic Energy Agency in Vienna, Austria.

The analytical precision was $\pm 0.1\text{‰}$ and $\pm 2\text{‰}$ for $\delta^{18}\text{O}$ and $\delta^2\text{H}$, respectively.

3.3. Data Analysis

Dansgaard (1964) introduced the concept of deuterium excess (d-excess), which is defined as $d = \delta^2\text{H} - 8\delta^{18}\text{O}$ [33]. The value of d-excess for precipitation is mainly associated with the meteorological conditions at the region from where the sample is derived, *i.e.*, the relative humidity in the atmosphere above the ocean, wind regime, ocean surface roughness, and temperature [34].

The hydrograph separation technique requires that the signatures of different water components be distinct and that the tracer signatures be conservative.

Stable isotope data have been used to estimate the quantities of the various water components that contribute to the groundwater [35–38]. The principle of these studies using stable isotopes is based on the contrast in the isotopic compositions of the water components. If there is no contrast between the water components, then a hydrograph separation using isotopes is not possible. Groundwater in the alpine region can be simply separated into two components of ice-snow meltwater and precipitation. $\delta^{18}\text{O}$ is an ideal index that is capable of hydrologic separation in the HLG watershed. A simple $\delta^{18}\text{O}$ -based hydrologic model may be applicable to estimate the relative contributions of hydrologic components over the total groundwater volume, as described below:

$$Q_G = Q_P + Q_{I-S} \quad (2)$$

where Q is the volumes of the mixing components, and the subscripts represent groundwater (G), precipitation (P), and ice-snow meltwater (I-S). Written then as an isotopic mass balance, it becomes:

$$Q_G \delta_G = Q_P \delta_P + Q_{I-S} \delta_{I-S} \quad (3)$$

where δ is the tracer concentration (isotope content). Thus, by substitution for $Q_P = Q_G - Q_{I-S}$ and rearranging:

$$f_{I-S} = \frac{Q_{I-S}}{Q_G} = \frac{(\delta_G - \delta_P)}{(\delta_{I-S} - \delta_P)} \quad \text{and} \quad f_P = 1 - f_{I-S} \quad (4)$$

where f is the fraction of the subscripted water components in groundwater. In order for this equation to be useful in calculating f , the requirements are that the isotopic parameters be different between the ice-snow meltwater and precipitation components and that the isotopes behave conservatively.

4. Results

4.1. Meteorological and Hydrological Characteristics

The hydro-meteorological data used in this study were collected in the HLG watershed. The precipitation and temperature were measured at the meteorological station (3000 m a.s.l.), which was located a short distance away from the stream water sampling site, and the water stage in the HLG river was measured at the hydrological station (2920 m a.s.l.), which was located approximately 1 km from the HLG glacier terminus (Figure 1). These two stations were established and maintained by the Gongga Mountain Alpine Ecosystem Station of the Chinese Academy of Sciences. Twenty-two years (1988–2009) of climatic data and 16 years (1994–2009) of hydrological data were collected in this study. Affected by the southeast monsoon, the eastern slope of Mount Gongga belongs to the wet monsoon climate of the subtropical mountains. It is calculated that the annual precipitation (at 3000 m a.s.l.) is over 1900 mm, with 20% of the annual total falling in the dry season (November–April) and 80% in the wet season (May–October), and the mean annual temperature is approximately 4.0 °C (Figure 2). Owing to the great rainfall and low evaporation, the water resources are very rich. The annual and inter-annual river flow change smoothly, and a steady baseflow exists even in the dry season. According to the results of the hydrological observation, the annual average discharge and runoff depth of the HLG River are approximately 7.8 m³/s and 3000 mm, respectively. The groundwater depth changes over time. During the dry season, the depth to the water table increases, and during the wet season, the depth to the water table decreases (Figure 2).

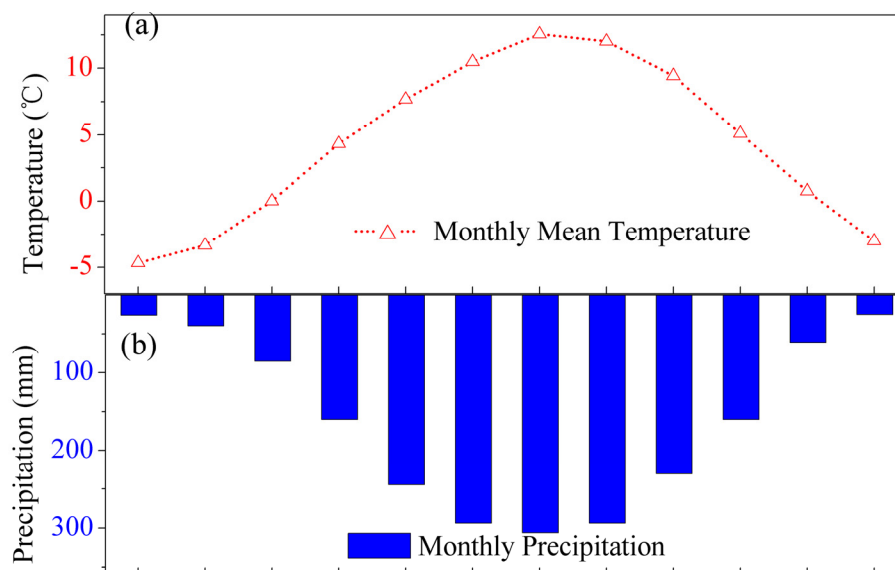


Figure 2. Cont.

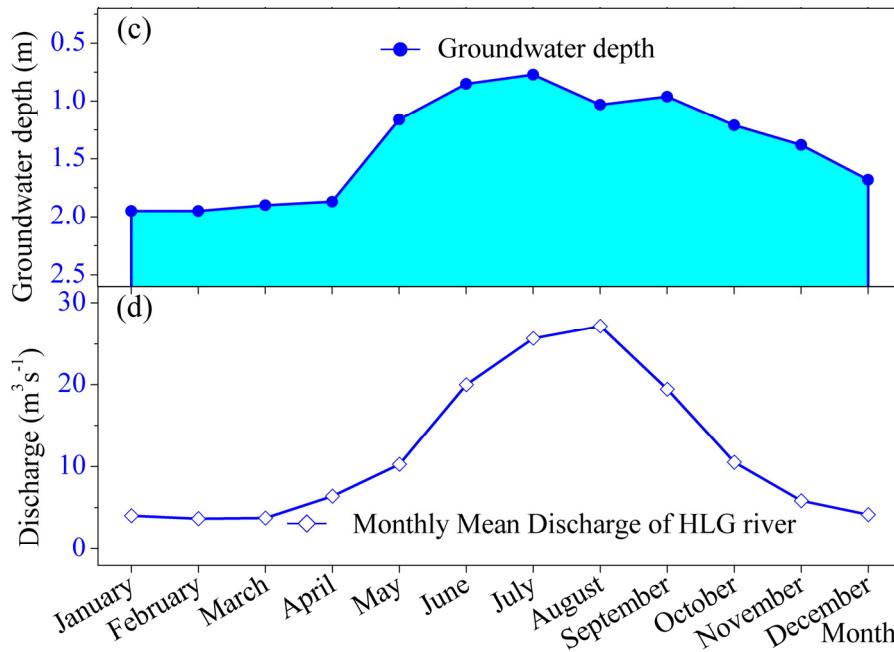


Figure 2. Seasonal variation of groundwater depth (m), temperature ($^{\circ}\text{C}$), precipitation (mm), and river runoff (m^3/s) at the HLG hydrological station: (a) the mean monthly temperature from 1988 to 2009; (b) the mean monthly precipitation from 1988 to 2009; (c) the groundwater depth during the observation period; and (d) the mean monthly discharge of the HLG River from 1994 to 2009.

4.2. Stable Isotopic Signatures of Water Samples

4.2.1. Isotopic Compositions of Water Samples

The statistics of the stable isotopic composition of the waters collected for this study are summarized in Table 1. Throughout the collection period from May 2008 to November 2009, 148 isotopic data of water samples were analyzed. The $\delta^{18}\text{O}$ and $\delta^2\text{H}$ values of the water samples display a marked seasonal variation (Figure 3). Maximum values were observed in the dry season months, with $\delta^{18}\text{O}$ and $\delta^2\text{H}$ as high as -3.7‰ and -23‰ , respectively. Minimum values were observed in the wet season months, with $\delta^{18}\text{O}$ and $\delta^2\text{H}$ as low as -15.3‰ and -108‰ , respectively. The groundwater shows a uniform isotopic signature, with $\delta^{18}\text{O}$ values between -13.5‰ and -11.1‰ and $\delta^2\text{H}$ values between -90‰ and -75‰ . Precipitation contains the widest range of isotopic variations, with the highest average values of $\delta^{18}\text{O}$ and $\delta^2\text{H}$ and the lowest d-excess values among all of the water sample categories. A clear seasonality, with lower $\delta^{18}\text{O}$ and $\delta^2\text{H}$ values of precipitation in the summer and higher values in the winter, is evident. The lowest values of $\delta^{18}\text{O}$ and $\delta^2\text{H}$ in precipitation were -15.3‰ and -109‰ , respectively; and the highest values were -3.7‰ and -23‰ , respectively. Overall, the ice-snow meltwater is isotopically most enriched in the heavy isotopes $\delta^{18}\text{O}$ and $\delta^2\text{H}$. The $\delta^{18}\text{O}$ values of ice-snow meltwater varied between -18.0‰ and -15.2‰ , and the $\delta^2\text{H}$ values varied between -123‰ and -101‰ .

Table 1. Statistics on isotopic compositions of groundwater, precipitation, and ice-snow meltwater in the study region.

Sample Type	Category	Minimum	Maximum	Annual Mean Value	Mean Value in Wet Season	Mean Value in Dry Season	
Groundwater	Site I	$\delta^{18}\text{O}(\text{‰})$	-13.5	-11.1	-12.2	-12.0	-12.4
		$\delta^2\text{H}(\text{‰})$	-90	-75	-81	-80	-83
		d-excess(‰)	13	19	16	16	16
	Site III	$\delta^{18}\text{O}(\text{‰})$	-12.9	-11.0	-11.9	-11.8	-12.2
		$\delta^2\text{H}(\text{‰})$	-88	-69	-79	-78	-82
		d-excess(‰)	12	20	16	16	16
Precipitation	Site I	$\delta^{18}\text{O}(\text{‰})$	-15.3	-3.7	-9.9	-10.5	-9.0
		$\delta^2\text{H}(\text{‰})$	-108	-23	-65	-71	-57
		d-excess(‰)	6	19	14	13	15
	Site II	$\delta^{18}\text{O}(\text{‰})$	-14.9	-6.2	-10.1	-10.3	-9.6
		$\delta^2\text{H}(\text{‰})$	-109	-39	-67	-69	-63
		d-excess(‰)	7	19	13	13	13
Ice-snow meltwater	$\delta^{18}\text{O}(\text{‰})$	-18.0	-15.2	-16.4	-16.4	-16.3	
	$\delta^2\text{H}(\text{‰})$	-123	-101	-110	-110	-109	
	d-excess(‰)	17	25	21	21	21	

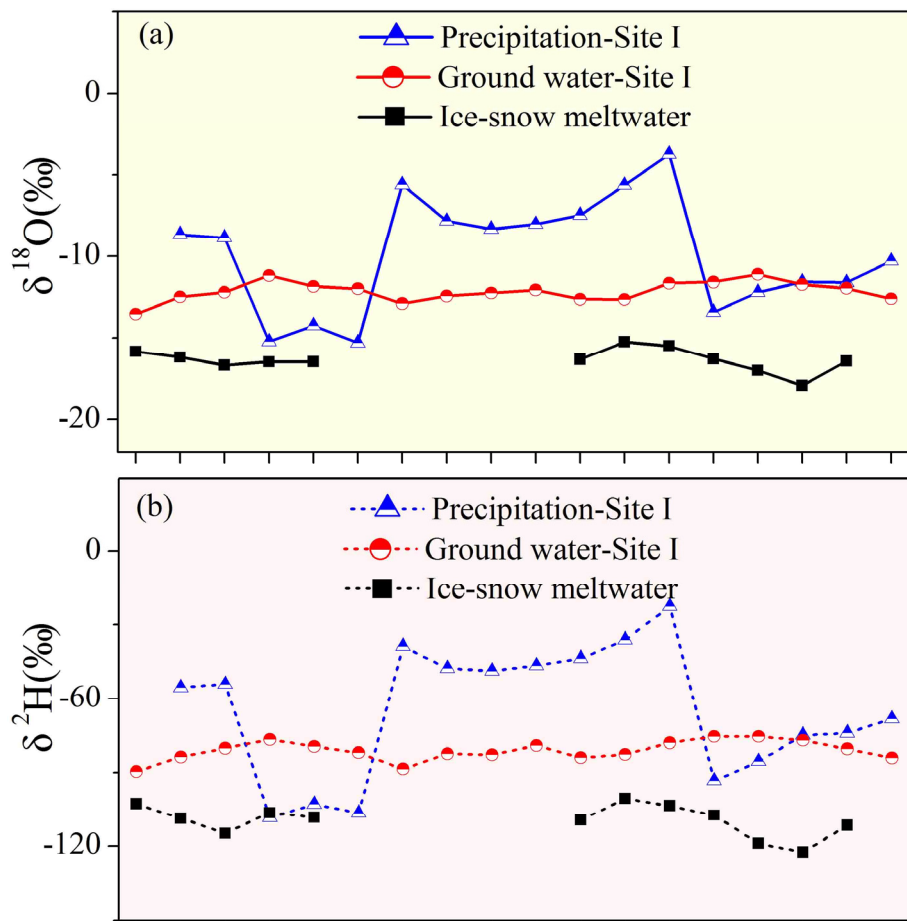


Figure 3. Cont.

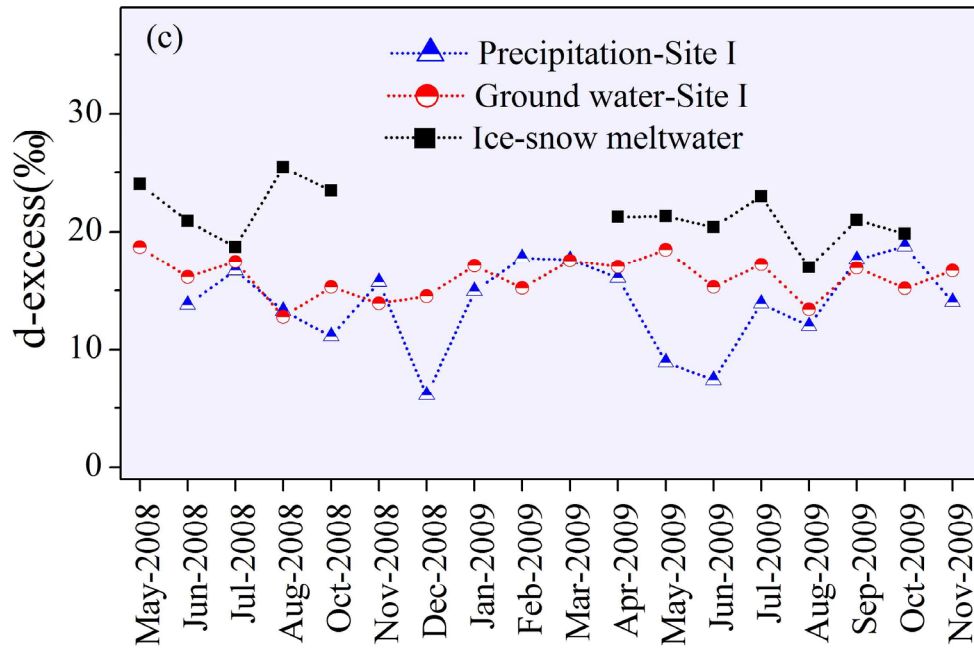


Figure 3. Temporal changes in $\delta^{18}\text{O}$ (a); $\delta^2\text{H}$ (b); and d-excess (c) of water samples in the study area.

4.2.2. Relationship between $\delta^{18}\text{O}$ and $\delta^2\text{H}$

The relationships between the $\delta^{18}\text{O}$ and $\delta^2\text{H}$ of precipitation, groundwater, and ice-snow meltwater collected in this investigation period are shown in Figure 4. The slope of the LMWL, which has been defined by the equation $\delta^2\text{H} = 7.8\delta^{18}\text{O} + 12.0\text{‰}$ ($R^2 = 0.981$) using the $\delta^{18}\text{O}$ and $\delta^2\text{H}$ values of the precipitation collected during this investigation period, is marginally lower than that of the GMWL. The linear correlations of the $\delta^{18}\text{O}$ and $\delta^2\text{H}$ values for the snowfall samples display higher slope and intercept values than those for the rainfall samples due to the influence of secondary evaporation [39]. Owing to snowfall events accounting for a relatively large portion of the annual total precipitation events and the low evaporation, the LMWL in the study region is characterized by slightly higher slope and intercept values (7.8 and 12.0) than those (7.3 and 5.6) of the LMWL for the Yangtze River basin [40]. The isotopic data points of the precipitation tend to be scattered along the LMWL (Figure 4), indicating large magnitudes of variation in $\delta^{18}\text{O}$ and $\delta^2\text{H}$. Many isotopic data points tend to fall in the upper end of the LMWL, which is interpreted to indicate the relatively large values of $\delta^{18}\text{O}$ and $\delta^2\text{H}$ of the precipitation (Figure 4).

The majority of the isotopic data points of groundwater fall close to the GMWL and LMWL, indicating that the evaporation effect on the isotopic variation of groundwater is very limited. This limited evaporation effect is due to the many foggy and cloudy days, lower temperature, large areas of forest, and the low wind velocity in this study region. Ice-snow meltwater is typically the most depleted in ^2H and ^{18}O in the study area. The stable isotopic compositions of water samples are summarized in Table 2.

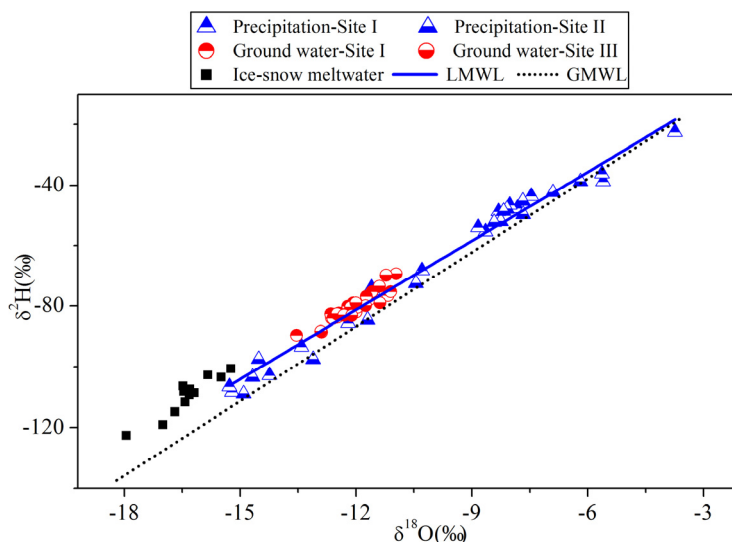


Figure 4. Correlation between $\delta^2\text{H}$ and $\delta^{18}\text{O}$ values for water collected from May 2008 to December 2009. The LMWL is shown as a solid line. The GMWL (dashed line) is shown for reference.

Table 2. The $\delta^{18}\text{O}$, $\delta^2\text{H}$, and d-excess values for water samples in the study region from May 2008 to November 2009.

Sample Type		Date	$\delta^{18}\text{O}(\text{‰})$	$\delta^2\text{H}(\text{‰})$	d-excess(‰)
Groundwater	Site I	8 June	-8.7	-55	14
		8 July	-8.8	-54	17
		8 August	-15.2	-108	13
		8 October	-14.2	-103	11
		8 November	-15.3	-107	16
		8 December	-5.6	-39	6
		9 January	-7.8	-48	15
		9 February	-8.3	-49	18
		9 March	-8.0	-47	18
		9 April	-7.5	-44	16
		9 May	-5.6	-36	9
		9 June	-3.7	-23	7
		9 July	-13.4	-93	14
		9 August	-12.2	-86	12
		9 September	-11.6	-75	18
9 October	-11.6	-74	19		
9 November	-10.3	-68	14		
Groundwater	Site III	8 June	-8.3	-52	14
		8 July	-8.1	-48	17
		8 August	-14.9	-109	10
		8 October	-14.5	-97	19
		8 November	-14.7	-103	14
		8 December	-6.9	-42	13
		9 February	-8.2	-49	17
9 April	-7.7	-50	12		

Table 2. Cont.

Sample Type	Date	$\delta^{18}\text{O}(\text{‰})$	$\delta^2\text{H}(\text{‰})$	d-excess(‰)	
Groundwater	Site III	9 May	-6.2	-39	11
		9 July	-13.1	-98	7
		9 August	-11.7	-85	9
		9 September	-7.7	-45	16
		9 October	-8.4	-52	15
Precipitation	Site I	8 May	-13.5	-90	19
		8 June	-12.5	-84	16
		8 July	-12.2	-80	17
		8 August	-11.2	-77	13
		8 October	-11.9	-80	15
		8 November	-12.0	-82	14
		8 December	-12.9	-89	15
		9 January	-12.4	-82	17
		9 February	-12.3	-83	15
		9 March	-12.1	-79	18
	9 April	-12.6	-84	17	
	9 May	-12.7	-83	19	
	9 June	-11.7	-78	15	
	9 July	-11.6	-75	17	
	9 August	-11.1	-75	13	
	9 September	-11.7	-77	17	
	9 October	-12.0	-81	15	
	9 November	-12.6	-84	17	
	Site II	8 June	-12.5	-83	17
		8 August	-11.0	-69	18
8 October		-11.8	-80	14	
8 November		-12.1	-81	17	
9 April		-12.3	-83	15	
9 May		-12.1	-83	14	
9 June		-11.4	-74	18	
9 July		-11.2	-70	20	
9 August		-12.0	-79	17	
9 September		-11.4	-79	12	
9 October	-12.9	-88	15		
Ice-snow meltwater	8 May	-15.8	-103	24	
	8 June	-16.2	-109	21	
	8 July	-16.7	-115	19	
	8 August	-16.5	-106	25	
	8 October	-16.5	-108	23	
	9 April	-16.3	-109	21	
	9 May	-15.2	-101	21	
	9 June	-15.5	-104	20	
	9 July	-16.3	-107	23	
	9 August	-17.0	-119	17	
	9 September	-18.0	-123	21	
9 October	-16.4	-112	20		

4.2.3. Characteristics of d-excess

Figure 3c show the variations in the d-excess of waters collected in the HLG watershed during the investigation period. There is a marked seasonal variation in the d-excess values of precipitation (Figure 3c), while the d-excess values of groundwater and ice-snow meltwater both show a relatively uniform signature (Figure 3c). This pattern of variability in the d-excess of groundwater may be explained by the attenuation of the seasonal d-excess signal of precipitation during infiltration. The precipitation contains relatively low values of d-excess, the groundwater contains relatively intermediate values of d-excess, and the ice-snow meltwater contains relatively high values of d-excess. This result indicates that (1) there is a significant inverse correlation between the d-excess value and the values of $\delta^{18}\text{O}$ and $\delta^2\text{H}$ for the water samples collected; (2) the d-excess features of groundwater can be explained by the input of ice-snow meltwater with relatively high values of d-excess in addition to precipitation; and (3) the d-excess signal of groundwater may be induced by different fractions of water component inputs in groundwater, instead of watershed-related evaporative enrichment or “evaporated” precipitation.

5. Discussion

5.1. Comparing Groundwater with Precipitation

Figure 3 shows a comparison of the isotopic composition of water samples collected in the observation period. There is a marked seasonal variation of $\delta^{18}\text{O}$ and $\delta^2\text{H}$ values, with minima in the wet season months and maxima in the dry season months. Due to the influence of the southeast monsoon, the intra-annual distribution of precipitation is relatively concentrated in the wet season (May–October, the main ablation period). This negative correlation between $\delta^{18}\text{O}$ and precipitation can be interpreted to indicate the so-called amount effect [33], a linear relationship between the decreasing stable isotopic values with the increasing amount of precipitation. It is evident that ice-snow meltwater is the most depleted in ^{18}O and ^2H in the study area.

Several important implications arise out of comparing the isotopic composition of groundwater with that of precipitation. Apparently, the seasonal isotopic variations observed in precipitation are substantially smoothed during the formation of groundwater. At sampling site I, seasonal $\delta^{18}\text{O}$ and $\delta^2\text{H}$ variations in groundwater have been attenuated to less than 21.2% and 16.4%, respectively, of those observed for precipitation; and, at sampling site III, the seasonal $\delta^{18}\text{O}$ and $\delta^2\text{H}$ variations have been attenuated to less than 16.9% and 22%, respectively.

The relationship between $\delta^{18}\text{O}$ and $\delta^2\text{H}$ of precipitation, groundwater, and ice-snow meltwater in the study area is shown in Figure 5. A comparison of the isotopic values of $\delta^{18}\text{O}$ and $\delta^2\text{H}$ for groundwater with those of precipitation shows that groundwater is more depleted in ^{18}O and ^2H than precipitation, suggesting that there are seasonal biases to the recharge and that the groundwater in this region may contain a common origin of heavy-isotope-depleted water (ice-snow meltwater) in addition to precipitation.

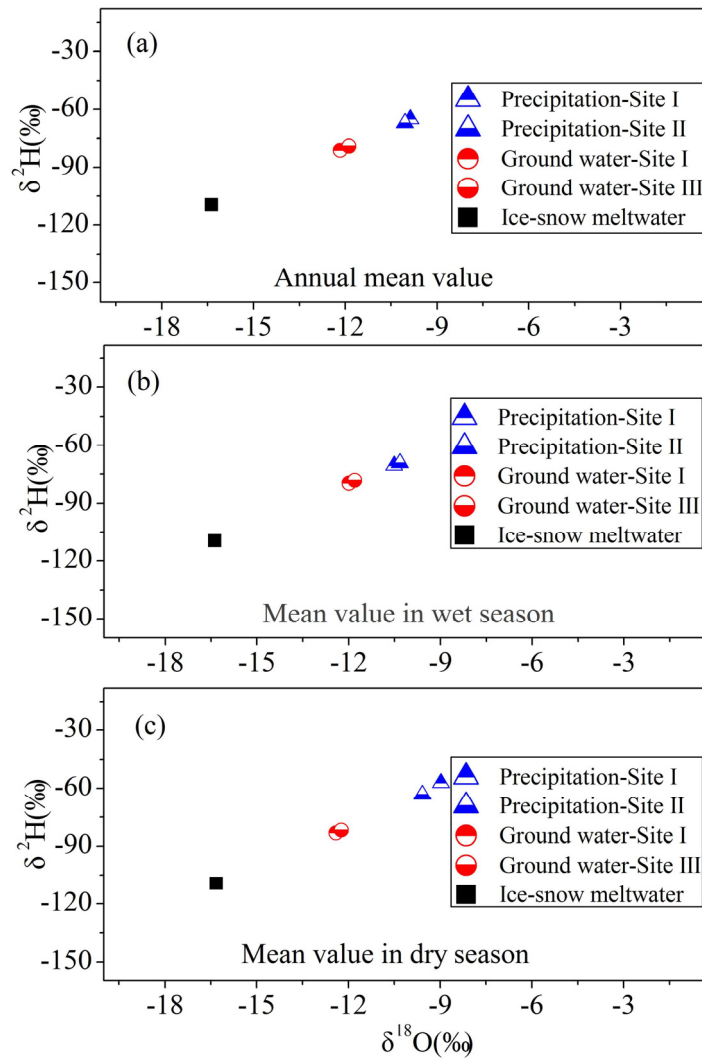


Figure 5. Relationships of $\delta^2\text{H}$ and $\delta^{18}\text{O}$ in precipitation, groundwater, and ice-snow meltwater: (a) annual mean value; (b) mean value in wet season; and (c) mean value in dry season.

Many processes may potentially affect the isotopic composition of groundwater in the study area:

(1) Much precipitation is lost by runoff and evapotranspiration in the study alpine region, and only part of the precipitation infiltrates to the water table, which could cause a seasonal bias in the isotopic composition of the groundwater. In the spring, when temperatures are low, vegetation is inactive and soils are saturated, the recharge rates from precipitation are generally high; in the summer, the recharge rate from precipitation is low because the most precipitation is evapotranspired back to the atmosphere; in the fall, the recharge rate from precipitation increases again due to the shut-down of photosynthesis; and in the winter, the frost precludes recharge in the study area.

(2) Ice-snow meltwater imparts an isotopic depletion to the groundwater recharge in this glacierized region. Ice-snow meltwater is a substantially important water source in this alpine glacierized area and is one of the two main sources of groundwater. The infiltration of meltwater in recharge is of great importance, requiring serious consideration in the pro-glacial region.

(3) There is no evidence for an evaporative component in groundwater. Evaporation is a systematic enrichment of the isotopic content of ^{18}O and ^2H relative to the composition of the original

precipitation [41]. On the basis of climate data (at 3000 m a.s.l.) from 1988 to 2009, it is calculated that the annual precipitation (at 3000 m a.s.l.) is over 1900 mm, but the annual evaporation is only approximately 300 mm in the HLG watershed. This result indicates that abundant precipitation and low evaporation are distinct climatic features in the study region, and so the evaporation has little effect on the isotopic composition of groundwater.

5.2. Groundwater Mixing in the Study Region

Clear deviations in the isotopic composition of groundwater from that of precipitation are found in this alpine glacierized region. There is an inverse trend of isotopic variation, in that the groundwater samples are isotopically more enriched in the heavy isotopes ^{18}O and ^2H in the wet season than in the dry season, while the precipitation samples are more depleted in the wet season than in the dry season. This inverse trend can be explained by the different fractions of water components in groundwater. As a whole, the groundwater is more depleted in the heavy isotopes ^{18}O and ^2H than the precipitation, whereas it is more enriched than the ice-snow meltwater. It is always desirable to estimate the various water components that contribute to groundwater. Groundwater in the study region mainly results from the percolation of precipitation and ice-snow meltwater [42]. The relative contributions of ice-snow meltwater and precipitation to the groundwater volume may be estimated by Equation (4).

Figure 6 shows the percentages of ice-snow meltwater and precipitation that contribute to groundwater at site I and site III, highlighting a marked seasonal variation. Specifically, we compare the calculated percentages of the water components based on $\delta^{18}\text{O}$ values with those based on $\delta^2\text{H}$ values. According to the $\delta^{18}\text{O}$ data on water collected in this investigation period, at site I, the calculated fraction of ice-snow meltwater is 35% on average over the year—that is, 33% in the wet season and 39% in the dry season—and that of precipitation is 65% (67% in the wet season and 61% in the dry season) (Figure 6a). And according to the $\delta^2\text{H}$ data, at site I, the calculated fraction of ice-snow meltwater is 36% on average over the year—that is, 33% in the wet season and 40% in the dry season—and that of precipitation is 64% (67% in the wet season and 60% in the dry season) (Figure 6b). According to the $\delta^{18}\text{O}$ data, at site III, the calculated fraction of ice-snow meltwater is 31% on average over the year—that is, 30% in the wet season and 36% in the dry season—and that of precipitation is 69% (70% in the wet season and 64% in the dry season) (Figure 6c). And according to the $\delta^2\text{H}$ data, at site III, the calculated fraction of ice-snow meltwater is 31% on average over the year—that is, 29% in the wet season and 38% in the dry season—and that of precipitation is 69% (71% in the wet season and 62% in the dry season) (Figure 6d). The results of this calculation on the basis of $\delta^{18}\text{O}$ are in line with those on the basis of $\delta^2\text{H}$, and the groundwater at site I is slightly more dominated by precipitation than that at site III. The results of this simple calculation attest to the fact that (1) groundwater in this alpine glacierized region is dominated by recharge from precipitation and ice-snow meltwater; (2) ice-snow meltwater plays an important role in the recharge of groundwater; and (3) the isotopic composition of groundwater is temporally variable, depending mainly on its sampling time.

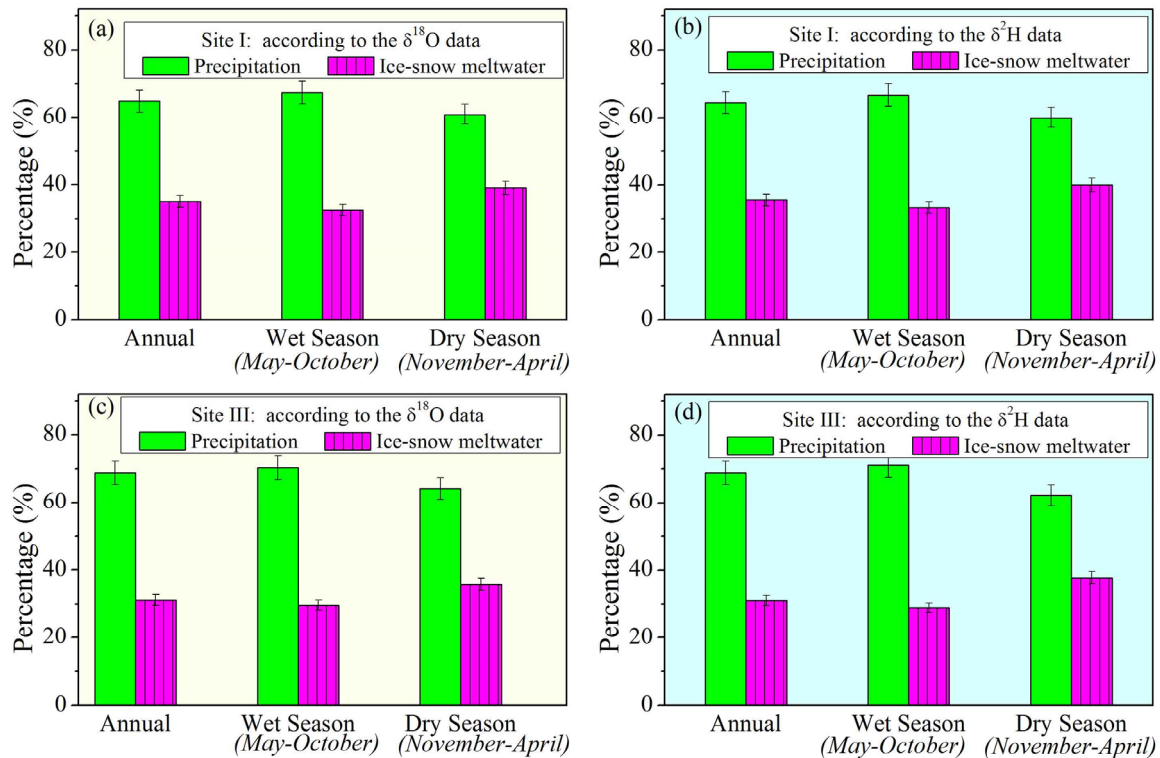


Figure 6. Calculated fractions of ice-snow meltwater and precipitation contributing to groundwater at sampling site I and site III: (a) site I, on the basis of $\delta^{18}\text{O}$; (b) site I, on the basis of $\delta^2\text{H}$; (c) site III, on the basis of $\delta^{18}\text{O}$; (d) site III, on the basis of $\delta^2\text{H}$.

6. Conclusions

The groundwater in the HLG watershed is generally a mixture of ice-snow meltwater and precipitation, with distinct isotopic compositions. Groundwater shows a uniform isotopic signature, and relatively intermediate values of $\delta^{18}\text{O}$, $\delta^2\text{H}$, and d-excess. Ice-snow meltwater is isotopically most enriched in the heavy isotopes $\delta^{18}\text{O}$ and $\delta^2\text{H}$ and contains the highest mean d-excess value. Precipitation contains the widest range of isotopic variation, the highest average values of $\delta^{18}\text{O}$ and $\delta^2\text{H}$, and the lowest d-excess value. On the basis of the relationship between $\delta^2\text{H}$ and $\delta^{18}\text{O}$, the majority of the isotopic data points of the groundwater fall close to the LMWL, indicating that the evaporation effect on the isotopic variation of groundwater is very limited. Given the small percentage of precipitation that becomes groundwater and this seasonal bias in recharge, the seasonal isotopic variations observed in precipitation are substantially attenuated during the formation of groundwater.

The groundwater in this alpine glacierized region is dominated by recharge from precipitation and ice-snow meltwater. Using a simple $\delta^{18}\text{O}$ model, we estimate that the fraction of ice-snow meltwater in the total groundwater volume is 35% and that of precipitation is 65% over the course of the year. The results of this study further demonstrate that ice-snow meltwater is a substantially important water source of groundwater in the alpine glacierized region and that stable isotopes are applicable to hydrological investigations.

Acknowledgments

This study was supported by the Youth Foundation of Sichuan University (Grant No. 2015SCU11048) and the Key Projects of Natural Science Foundation of China (Grant No. 40730634). The authors are grateful to the Gongga Mountain Alpine Ecosystem Station, Chengdu Institute of Mountain Hazards and Environment, and the Chinese Academy of Sciences, Sichuan, China, for supplying necessary meteorological data.

Author Contributions

All authors contributed extensively to the work presented in this paper. Yuchuan Meng conceived the research, wrote the manuscript, revised, and finalized the paper. Guodong Liu conceived the research and processed all the data. MingXi Li conceptualized and supervised the research.

Conflicts of Interest

The authors declare no conflict of interest.

References

1. Beniston, M. Climatic change in mountain regions: A review of possible impacts. *Clim. Chang.* **2003**, *59*, 5–31.
2. Deng, M.Z.; Qin, D.H.; Zhang, H.G. Public perceptions of climate and cryosphere change in typical arid inland river areas of China: Facts, impacts and selections of adaptation measures. *Quat. Int.* **2012**, *282*, 48–57.
3. Salama, M.S.; van der Velde, R.; Zhong, L.; Ma, Y.; Ofwono, M.; Su, Z. Decadal variations of land surface temperature anomalies observed over the Tibetan Plateau by the special sensor microwave imager (SSM/I) from 1987 to 2008. *Clim. Chang.* **2012**, *114*, 769–781.
4. Li, Z.X.; He, Y.Q.; Wang, C.F.; Wang, X.F.; Xin, H.J.; Zhang, W.; Cao, W.H. Spatial and temporal trends of temperature and precipitation during 1960–2008 at the Hengduan Mountains, China. *Quat. Int.* **2011**, *236*, 127–142.
5. Dedieu, J.P.; Lessard-Fontaine, A.; Ravazzani, G.; Cremonese, E.; Shalpykova, G.; Beniston, M. Shifting mountain snow patterns in a changing climate from remote sensing retrieval. *Sci. Total Environ.* **2014**, *493*, 1267–1279.
6. Parish, R.; Funnell, D.C. Climate change in mountain regions: Some possible consequences in the Moroccan High Atlas. *Glob. Environ. Chang.* **1999**, *9*, 45–48.
7. Bauder, A.; Funk, M.; Huss, M. Ice-volume changes of selected glaciers in the Swiss Alps since the end of the 19th century. *Ann. Glaciol.* **2007**, *46*, 145–149.
8. Lambrecht, A.; Kuhn, M. Glacier changes in the Austrian Alps during the last three decades, derived from the new Austrian glacier inventory. *Ann. Glaciol.* **2007**, *46*, 177–184.
9. Lambrecht, A.; Mayer, C. Temporal variability of the non-steady contribution from glaciers to water discharge in western Austria. *J. Hydrol.* **2009**, *376*, 353–361.

10. Baraer, M.; Mark, B.G.; McKenzie, J.M.; Condom, T.; Bury, J.; Huh, K.I.; Portocarrero, C.; Gomez, J.; Rathay, S. Glacier recession and water resources in Peru's Cordillera Blanca. *J. Glaciol.* **2012**, *58*, 134–150.
11. Barnett, T.P.; Adam, J.C.; Lettenmaier, D.P. Potential impacts of a warming climate on water availability in snow-dominated regions. *Nature* **2005**, *438*, 303–309.
12. Immerzeel, W.W.; van Beek, L.P.H.; Bierkens, M.F.P. Climate change will affect the Asian water towers. *Science* **2010**, *328*, 1382–1385.
13. Rees, H.G.; Collins, D.N. Regional differences in response of flow in glacier-fed Himalayan rivers to climatic warming. *Hydrol. Process* **2006**, *20*, 2157–2169.
14. Marshall, S.J.; White, E.C.; Demuth, M.N.; Bolch, T.; Wheate, R.; Menounos, B.; Beedle, M.J.; Shea, J.M. Glacier Water Resources on the Eastern Slopes of the Canadian Rocky Mountains. *Can. Water Resour. J.* **2011**, *36*, 109–133.
15. Finger, D.; Hugentobler, A.; Huss, M.; Voinesco, A.; Wernli, H.; Fischer, D.; Weber, E.; Jeannin, P.Y.; Kauzlaric, M.; Wirz, A.; *et al.* Identification of glacial meltwater runoff in a karstic environment and its implication for present and future water availability. *Hydrol. Earth Syst. Sci.* **2013**, *17*, 3261–3277.
16. Zhao, H.X.; Moore, G.W.K. On the relationship between Tibetan snow cover, the Tibetan plateau monsoon and the Indian summer monsoon. *Geophys. Res. Lett.* **2004**, *31*, doi:10.1029/2004GL020040.
17. Heim, A. The glaciation and solifluction of Minya Gongka. *Geogr. J.* **1936**, *87*, 444–454.
18. He, Y.Q.; Li, Z.X.; Yang, X.M.; Jia, W.X.; He, X.Z.; Song, B.; Zhang, N.N.; Liu, Q. Changes of the Hailuoguo Glacier, Mt Gongga, China, against the background of global warming in the last several decades. *J. China Univ. Geosci.* **2008**, *19*, 271–281.
19. Li, Z.X.; He, Y.Q.; Yang, X.M.; Theakstone, W.H.; Jia, W.X.; Pu, T.; Liu, Q.; He, X.Z.; Song, B.; Zhang, N.N.; *et al.* Changes of the Hailuoguo glacier, Mt. Gongga, China, against the background of climate change during the Holocene. *Quat. Int.* **2010**, *218*, 166–175.
20. Pan, B.T.; Zhang, G.L.; Wang, J.; Cao, B.; Geng, H.P.; Wang, J.; Zhang, C.; Ji, Y.P. Glacier changes from 1966 to 2009 in the Gongga Mountains, on the south-eastern margin of the Qinghai-Tibetan Plateau and their climatic forcing. *Cryosphere* **2012**, *6*, 1087–1101.
21. Meng, Y.C.; Liu, G.D.; Zhang, L.T. A comparative study on stable isotopic composition in waters of the glacial and nonglacial rivers in Mount Gongga, China. *Water Environ. J.* **2014**, *28*, 212–221.
22. Craig, H. Isotope variations in meteoric waters. *Science* **1961**, *133*, 1702–1703.
23. Rozanski, K.; Araguas-Araguas, L.; Gonfiantini, R. Isotopic pattern in modern global precipitation. In *Climatic Change in Continental Isotopic Records*, 1st ed.; Swart, P.K., Lohwan, K.L., Mckenzie, J., Savin, S., Eds.; Geophysical Monograph No 78, American Geophysical Union: Washington, DC, USA, 1993; Volume 1, pp. 1–37.
24. Kristiansen, S.M.; Yde, J.C.; Bárcena, T.G.; Jakobsen, B.H.; Olsen, J.; Knudsen, N.T. Geochemistry of groundwater in front of a warm-based glacier in Southeast Greenland. *Geogr. Ann. Ser. A Phys. Geogr.* **2013**, *95*, 97–108.
25. Wadham, J.L.; Cooper, R.J.; Tranter, M.; Bottrell, S. Evidence for widespread anoxia in the proglacial zone of an Arctic glacier. *Chem. Geol.* **2007**, *243*, 1–15.
26. Blaen, P.J.; Hannah, D.M.; Brown, L.E.; Milner, A.M. Water temperature dynamics in High Arctic river basins. *Hydrol. Process.* **2013**, *27*, 2958–2972.

27. Tan, H.B.; Rao, W.B.; Chen, J.S.; Su, Z.G.; Sun, X.X.; Liu, X.Y. Chemical and isotopic approach to groundwater cycle in western Qaidam Basin, China. *Chin. Geogr. Sci.* **2009**, *19*, 357–364.
28. Thomas, A. Overview of the geocology of the Gongga Shan range, Sichuan province, China. *Mt. Res. Dev.* **1999**, *17*, 17–30.
29. Thomas, A. The climate of the Gongga Shan range, Sichuan Province, PR China. *Arct. Alpine Res.* **1997**, *29*, 226–232.
30. Shen, Z.; Lui, Z.; Fank, J. Altitudinal changes in species diversity and community structure of *Abies fabri* communities at Hailuo Valley of Mt. Gongga, Sichuan. *Biodivers. Sci.* **2004**, *12*, 237–244. (In Chinese)
31. Zhang, Y.; Fujita, K.; Liu, S.Y.; Liu, Q.A.; Wang, X. Multi-decadal ice-velocity and elevation changes of a monsoonal maritime glacier: Hailuogou glacier, China. *J. Glaciol.* **2010**, *56*, 65–74.
32. Liu, Q.A.; Liu, S.Y.; Zhang, Y.; Wang, X.; Zhang, Y.S.; Guo, W.Q.; Xu, J.L. Recent shrinkage and hydrological response of Hailuogou glacier, a monsoon temperate glacier on the east slope of Mount Gongga, China. *J. Glaciol.* **2010**, *56*, 215–224.
33. Dansgaard, W. Stable isotopes in precipitation. *Tellus* **1964**, *16*, 436–468.
34. Merlivat, M.; Jouzel, J. Global climatic interpretation of the deuterium–oxygen-18 relationship for precipitation. *Geophys. Res.* **1979**, *84*, 5029–5033.
35. Buttle, J.M. Isotope hydrograph separations and rapid delivery of pre-event water from drainage basins. *Prog. Phys. Geog.* **1994**, *18*, 16–41.
36. Iacumin, P.; Venturelli, G.; Selmo, E. Isotopic features of rivers and groundwater of the Parma Province (Northern Italy) and their relationships with precipitation. *J. Geochem. Explor.* **2009**, *102*, 56–62.
37. Jeelani, G.; Bhat, N.A.; Shivanna, K. Use of $\delta^{18}\text{O}$ tracer to identify stream and spring origins of a mountainous catchment: A case study from Liddar watershed, Western Himalaya, India. *J. Hydrol.* **2010**, *393*, 257–264.
38. Chiogna, G.; Santoni, E.; Camin, F.; Tonon, A.; Majone, B.; Trenti, A.; Bellin, A. Stable isotope characterization of the Vermigliana catchment. *J. Hydrol.* **2014**, *509*, 295–305.
39. Peng, H.D.; Mayer, B.; Harris, S.; Krouse, H. A 10-yr record of stable isotope ratios of hydrogen and oxygen in precipitation at Calgary, Alberta, Canada. *Tellus B* **2004**, *56*, 147–159.
40. Meng, Y.C.; Liu, G.D. The Below-cloud Secondary Evaporation Effects on the Stable Isotope Composition in Precipitation in Yangtze River Basin. *Adv. Water Sci.* **2010**, *21*, 327–334. (In Chinese)
41. Gat, J.R. Oxygen and hydrogen isotopes in the hydrological cycle. Annual Review of Earth Planetary. *Sciences* **1996**, *24*, 225–262.
42. Cao, Z.T.; Cheng, G.W. Preliminary analysis of hydrological characteristics of Hailuogou glacier on the eastern slope of the Gongga Mountain. In *Glaciers and Environment in the QinghaiXizang (Tibet) Plateau, [1]—The Gongga Mountain*, 1st ed.; Xie, Z.C., Kotlyakov, V.M., Eds.; Science Press: Beijing, China, 1994; Volume 1, pp. 143–156.